Cell

An Interdomain Energetic Tug-of-War Creates the Allosterically Active State in Hsp70 Molecular Chaperones

Anastasia Zhuravleva,[1] Eugenia M. Clerico,[1] and Lila M. Gierasch[1,2,*]
[1]Department of Biochemistry and Molecular Biology
[2]Department of Chemistry
University of Massachusetts, Amherst, MA 01003, USA
*Correspondence: gierasch@biochem.umass.edu
http://dx.doi.org/10.1016/j.cell.2012.11.002

SUMMARY

The allosteric mechanism of Hsp70 molecular chaperones enables ATP binding to the N-terminal nucleotide-binding domain (NBD) to alter substrate affinity to the C-terminal substrate-binding domain (SBD) and substrate binding to enhance ATP hydrolysis. Cycling between ATP-bound and ADP/substrate-bound states requires Hsp70s to visit a state with high ATPase activity and fast on/off kinetics of substrate binding. We have trapped this "allosterically active" state for the *E. coli* Hsp70, DnaK, and identified how interactions among the NBD, the β subdomain of the SBD, the SBD α-helical lid, and the conserved hydrophobic interdomain linker enable allosteric signal transmission between ligand-binding sites. Allostery in Hsp70s results from an energetic tug-of-war between domain conformations and formation of two orthogonal interfaces: between the NBD and SBD, and between the helical lid and the β subdomain of the SBD. The resulting energetic tension underlies Hsp70 functional properties and enables them to be modulated by ligands and cochaperones and "tuned" through evolution.

INTRODUCTION

The 70 kDa heat shock proteins (Hsp70s) are ubiquitous molecular chaperones that mediate a broad array of critical cellular functions integral to protein homeostasis (Calloni et al., 2012; Hartl et al., 2011; Mayer and Bukau, 2005; Mayer et al., 2001). Allosteric signals in Hsp70s initiate from ligand binding events—nucleotide and substrate—and are further modulated by cochaperones (Figure 1A). Upon binding of ATP to the N-terminal 45 kDa actin-like nucleotide-binding domain (NBD), the affinity of the C-terminal 30 kDa substrate-binding domain (SBD) for substrates decreases by up to two orders of magnitude as compared to its affinity in the absence of nucleotide or when the NBD is bound to ADP (Figure S1A available online). In turn, substrate binding to the SBD stimulates the ATPase activity of the NBD (Figure S1B). These allosteric changes are reversible, and the resulting cycle of substrate binding/release, nucleotide hydrolysis, and nucleotide exchange repeats with a timing that is regulated by the availability and affinity of substrates, ATP/ADP balance, and cochaperone interactions.

The structural origin of allosteric signal transmission within and between Hsp70s domains remains poorly understood. In ADP-bound DnaK, the *Escherichia coli* Hsp70, which is the best-studied Hsp70 from a biophysical perspective, the NBD and SBD are largely independent and behave as "beads on a string" (Bertelsen et al., 2009; Swain et al., 2007), retaining the structures they adopt as isolated domains (Flaherty et al., 1990; Zhu et al., 1996) (Figure 1B). Upon ATP binding, the two domains rearrange to an intimately packed and dramatically reorganized domain-docked structure (Mapa et al., 2010; Marcinowski et al., 2011; Swain et al., 2007; Wilbanks et al., 1995). Although the atomic structure of an ATP-bound domain-docked Hsp70 has not yet been reported, the recently described structure of an Hsp70 homolog, yeast Hsp110, Sse1, bound to ATP (Liu and Hendrickson, 2007) has provided a good model for the domain-docked ATP-bound conformation of an Hsp70 (Figure 1C). The domain rearrangements of ATP-bound DnaK deduced from a homology model based on the structure of ATP-bound Hsp110 are consistent with observed ATP-induced conformational changes (Buchberger et al., 1995; Mapa et al., 2010; Rist et al., 2006; Wilbanks et al., 1995), with the effects of several known mutations (Liu and Hendrickson, 2007), and with a recent analysis of residue coevolution (Smock et al., 2010). The structural models for the ADP- and ATP-bound states implicate very large rigid body reorientations and altered arrangements of the NBD, the β subdomain of the SBD, and α-helical lid subdomains (Figures 1B and 1C), with relatively small changes in internal subdomain structures in the ATP-induced Hsp70 allosteric conformational change (Figure S1C).

Understanding how ligands mediate the Hsp70 allosteric structural rearrangement demands deeper insight into the mechanism of this conformational transition. Specifically, there must be at least one intermediate state visited between the two "endpoint" states, undocked (ADP and substrate bound) and docked (ATP bound with no substrate), in the allosteric cycle of an Hsp70 (Figure 1A). Substrate binding enhances the rate of ATP hydrolysis by the NBD; hence, both substrate and ATP

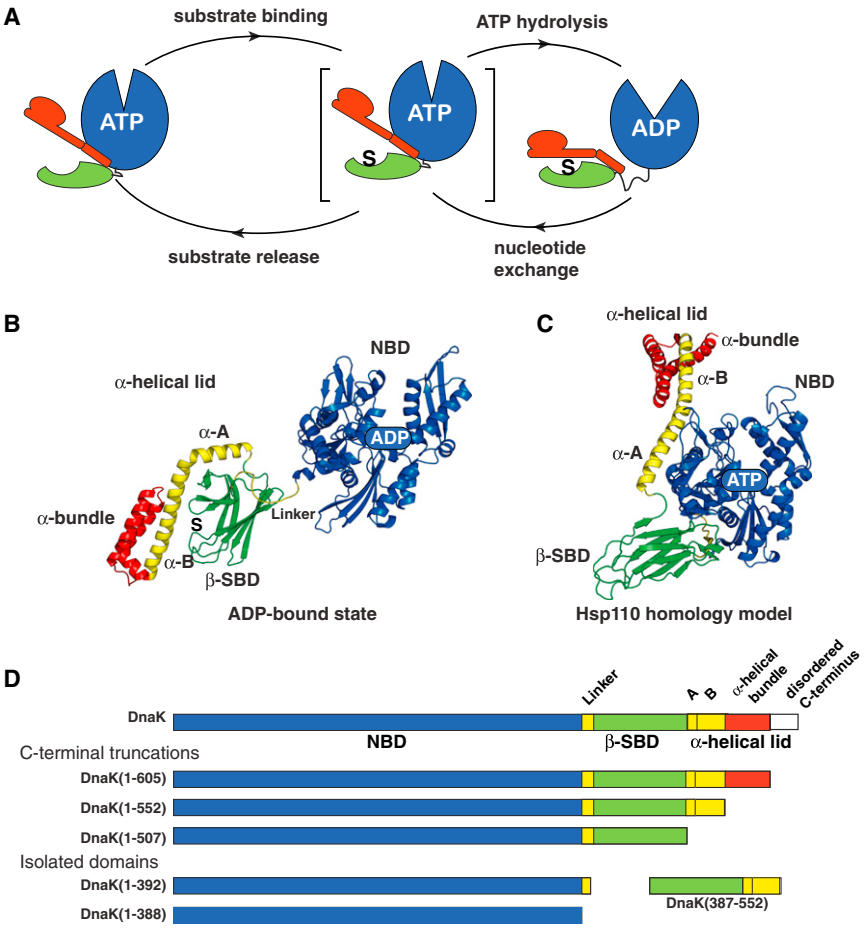

Figure 1. Conformational Insights into the Hsp70 Allosteric Cycle

(A) The Hsp70 allosteric cycle. S, substrate.

(B and C) Ribbon representation of the structures of the two "endpoint" states of DnaK: the ADP-bound state (PDB 2kho), and the Hsp110-based homology model of the ATP-bound state (Smock et al., 2010; coordinates available upon request). Structural elements are colored as in (D). (See also Figure S1.)

(D) DnaK constructs used for NMR studies.

must bind to the intermediate, allosterically active state. Moreover, this intermediate is a tipping point between two "endpoint" states: on the one hand, ATP binding results in fast substrate unbinding and stabilizes the docked (substrate-unbound) state; on the other hand, substrate binding significantly enhances ATP hydrolysis, which then leads to the ADP-substrate bound (undocked) state. Provocatively, the presence of the SBD is not required for the NBD to adopt a conformation with stimulated ATPase activity. Indeed, binding of the highly conserved hydrophobic interdomain linker to the cleft beneath the crossing helices in an isolated NBD is necessary and sufficient for ATPase activation (Swain et al., 2007; Vogel et al., 2006).

How then does substrate binding lead to the population of an allosterically active conformation? And reciprocally, how does ATP-induced domain docking control substrate affinity? In this study, we address these questions through the use of a mutated DnaK that is impaired in ATP hydrolysis such that we can create a stable ATP/substrate-bound DnaK sample. To elucidate the interdomain allosteric mechanism of DnaK, we employed NMR spectroscopy as an extremely powerful tool to characterize the relationship between protein allostery and function (Manley and Loria, 2012; Tzeng and Kalodimos, 2011). The information we have obtained has allowed us to "dissect" allostery in DnaK and define the roles of different allosteric units—viz, the NBD, the β subdomain of the SBD or β-SBD, and the α-helical lid of the SBD (Figure 1). The tensions and balances among these allosteric units underlie the Hsp70 allosteric cycle and give rise to "tunability" in the Hsp70 system. Our results, gleaned from study of DnaK, have implications for sequence and function relationships in other Hsp70s and shed light on how cochaperones may modulate the Hsp70 allosteric cycle.

RESULTS

Methyl NMR Reveals Three Distinct Hsp70 Conformational Ensembles: Two Endpoint States and an Intermediate

To explore ligand-induced allosteric transitions for the full-length 70 kDa DnaK, we employed methyl transverse relaxation optimized spectroscopy (methyl-TROSY) (Tugarinov et al., 2003), which is a powerful and sensitive method to probe protein conformations of large proteins with atomic resolution (Ruschak and Kay, 2010; Tugarinov and Kay, 2005). Consistent with previous results based on ^{1}H-^{15}N HSQC spectra (Swain et al., 2007), isoleucine methyl-TROSY spectra show few chemical shift changes between a two-domain DnaK construct, either apo (nucleotide-free) or ADP bound, and isolated NBD and SBD (Figures 2A and S2C). These data support the conclusion that the NBD and SBD of both nucleotide-free and ADP-bound DnaK lack significant interdomain interactions and behave as "beads on a string" that are connected by a solvent-exposed, highly flexible interdomain linker.

To "trap" DnaK in the ATP-bound state, we incorporated the T199A mutation, which blocks ATP hydrolysis and thus stabilizes the ATP-bound state without disruption of ATP-induced conformational changes (McCarty and Walker, 1991). Large chemical shift changes are observed between ATP-bound DnaK-T199A (which we will refer to as DnaK) and its isolated domains in corresponding ligand-bound states (Figure 2B), consistent with widespread conformational rearrangements in both domains upon ATP binding, as expected based on the Hsp110-based homology structure (Figure 1C). The perturbed chemical shifts may result from direct interactions between domains and/or

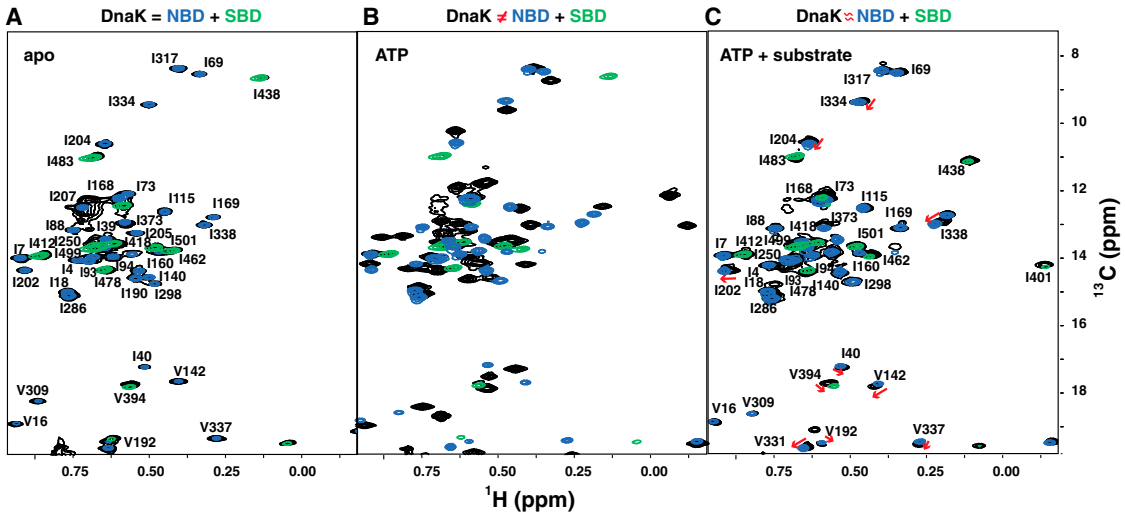

Figure 2. NMR Fingerprints of DnaK Reveal Three Different Ligand-Bound States in Its Allosteric Cycle

(A–C) The isoleucine region of methyl-TROSY spectra of the two-domain DnaK constructs (black indicates DnaK(1-552) in A and B and full-length DnaK in C; see Figure S2 for full-length DnaK in the ADP-bound state) are overlaid with the spectra of corresponding nucleotide and substrate-bound states of the individual domains: NBD, DnaK(1-388), is in blue, and SBD, DnaK(387-552), is in green. (A) Nucleotide free. (B) ATP bound. (C) ATP/substrate bound. In (C), red arrows point to small but significant chemical shift differences between NBD resonances of the full-length ATP/substrate-bound DnaK and those of its isolated NBD.

indirect long-range conformational changes. Strikingly, substrate binding to ATP-bound DnaK results in additional conformational changes (Figure 2C), which we discuss in detail below and conclude are critical to the allosteric function of DnaK.

Our methyl-TROSY NMR data on the different DnaK ligand-bound states reveal that this protein samples at least three conformations during its allosteric cycle (Figure 1A); these arise from distinct domain arrangements: the ADP-bound domain-undocked conformation (Figure 2A), the ATP-bound domain-docked conformation (Figure 2B), and the conformational ensemble populated in the presence of ATP and substrate (Figure 2C). We performed detailed characterization of the ATP-bound states—both the domain-docked and the conformational ensemble created in the presence of both ATP and substrate—to gain deeper insight into how transitions between them affect Hsp70 functions (ATP hydrolysis and substrate binding) and how nucleotide and substrate binding control these conformational transitions.

The ATP-Bound, Domain-Docked State of DnaK

To validate the Hsp110-based homology model of ATP-bound DnaK, we compared peak positions in HNCO spectra of the isolated NBD and two-domain DnaK constructs (Figures 3A and S3A). Figure 3A demonstrates that the NBD residues suffering significant changes in local environment between the ATP-bound NBD (DnaK(1-392)) and two-domain (DnaK(1-552)) constructs, as indicated either by chemical shift changes and/or altered microsecond-millisecond dynamics, are fully consistent with the NBD-SBD interfaces in the Hsp110-based model of ATP-bound DnaK. A pairwise chemical shift comparison between ATP-bound DnaK(1-552) and DnaK(1-507) constructs, the latter of which is truncated so as to lack the α-helical lid sequence, revealed perturbations to the NBD interface upon interaction with the α-helical lid (Figures 3B, significant perturbations shown in green, and S3A), in full agreement with the Hsp110-based homology model of ATP-bound DnaK.

To obtain a more detailed description of the interfaces formed in the ATP-bound state without causing long-range changes, we created "soft" mutations of residues involved in the NBD-β SBD and NBD-α-helical lid interfaces (Figure 3C). These mutations lead to local perturbations around the mutation site but do not perturb protein conformation (Figures S3B and S3C). Consequently, chemical shift perturbations in the NBD upon "soft" mutations in the β SBD or α-helical lid (Figures S3B and S3D) provide direct information about NBD-β-SBD or NBD-α-helical lid contacts in the ATP-bound states. The observed effects of several "soft" mutations are completely consistent with the predicted packing of the interdomain interfaces based on the Hsp110-based model (Figure 3C).

The observation of random coil-like chemical shifts (Figure S3E) and high-peak intensities (Figure S3F) for residues 520–546 of helix B of the α-helical lid in ATP-bound DnaK(1-552) argues that this region is mobile and significantly destabilized, in contrast to the Hsp110 structure. These results argue that upon ATP binding, the α-helical bundle detaches from the β-SBD and forms only transient contacts with the NBD. Our conclusion is consistent with hydrogen exchange mass spectrometry results that showed that the proximal part of helical lid helix B (from residue 512 to residue 532), but not the helical bundle, became unstructured upon ATP binding (Rist et al., 2006). To further check that lack of interaction of helix B with the NBD is real and not a truncation artifact arising from the absence of the α-helical bundle, we compared chemical shifts of the NBD and β-SBD in ATP-bound full-length DnaK and DnaK(1-605) (both with the full helical lid, the latter missing

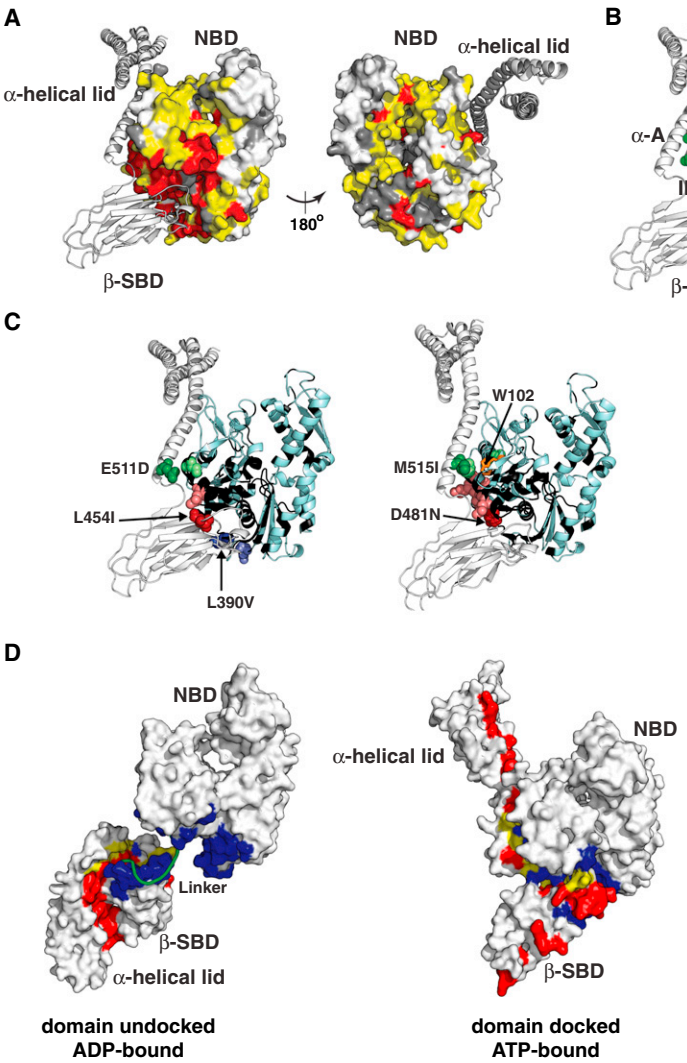

Figure 3. Experimental Validation of the Hsp110-Based Homology Model for the ATP-Bound, Domain-Docked State of DnaK

(A and B) Mapping of the NBD residues that were significantly affected by interaction with the β-SBD onto the structure of the Hsp110-based homology model. Residues with significant chemical shift differences (see text) between DnaK(1-552) and either DnaK(1-392) or DnaK(1-507) are shown in yellow and green, respectively. Residues showing enhanced microsecond-millisecond dynamics upon ATP binding, i.e., whose assignments were obtained for the isolated NBD but not for DnaK(1-552), are shown in red (see Extended Experimental Procedures). The unassigned residues in either construct are shown in dark gray; the rest are shown in light gray (see also Figure S3A).

(C) Ribbon representation of the Hsp110-based homology model showing effects of "soft" mutations on backbone (L454I, D481N, L390V, and E511D) and methyl (M515I) chemical shifts of ATP-bound (docked) DnaK(1-552). A site of mutation and the residues affected (see Extended Experimental Procedures) are shown as dark- and light-colored spheres, respectively (see also Figures S3B and S3C) Trp102, which becomes solvent exposed in the ADP-bound conformation of DnaK (Buchberger et al., 1995), is shown in orange sticks on right. NBD residues without backbone assignments are shown in black.

(D) Interfaces between the NBD, β-SBD and α-helical lid are shown mapped onto the two endpoint Hsp70 states, domain undocked/linker unbound (PDB 2kho) and domain docked (Hsp110-based homology model [see Experimental Procedures]): residues at the interface between the β-SBD and α-helical lid, which is stabilized by substrate binding, are in red, and residues at the interface between the NBD and either the β-SBD or the α-helical lid, which is stabilized upon cooperative ATP and linker binding, are in blue; residues participating in both interfaces are in yellow.

only the disordered C-terminal segment) and DnaK(1-552) (missing the helical bundle) and saw no significant differences. The picture that emerges is that ATP binding is accompanied by a partial unfolding of the proximal part of helix B of the helical lid, mobility of the lid around this flexible site, loss of interaction with the β-SBD, and no new stable interactions with the NBD.

Intriguingly, chemical shift differences between the ATP-bound two-domain protein, DnaK(1-552), and either the NBD (DnaK(1-392)) or SBD (DnaK(387-552)) are greater than 0.2, 1, and 0.5 ppm for ^{1}HN, ^{15}N, and ^{13}CO atoms, respectively, and include residues distant from the interdomain interfaces, which is not consistent with solely rigid body rearrangements of the NBD, β-SBD, and α-helical bundle, as predicted from the Hsp110-based homology model. In particular, significant perturbations are observed at the nucleotide-binding site of the NBD (Figure S3A), and dramatic, widespread changes are observed throughout the β-SBD (Figures S3G and S3H). Such changes cannot be explained by local effects of interdomain docking or α-helical lid removal (Figure S3I) and point to extensive conformational changes everywhere in the β-SBD, including in the substrate-binding site.

Thus, our experimental data for ATP-bound DnaK argue that the Hsp110 homology model correctly describes relative arrangements of the NBD, β-SBD, and α-helical bundle and define the NBD-β-SBD and NBD-α-helical lid interfaces in the docked conformation but fails to capture long-range conformational changes inside Hsp70 domains. Intriguingly, the two "endpoint" Hsp70 conformations, domain undocked (ADP bound) and domain docked (ATP bound), have orthogonal patterns of interactions between the NBD, β-SBD and α-helical lid, including α-helical lid interaction with the β-SBD in the undocked state (red in Figure 3D), and NBD-β-SBD interaction in the docked state (blue in Figure 3D). These orthogonal interfaces can be expected to compete energetically when factors such as ligand binding differentially stabilize them (see below).

Binding of Substrate to ATP-Bound DnaK Leads to Domain Dissociation with Interdomain Linker Binding: The Allosterically Active State

The key allosteric functions of an Hsp70 machine require that the binding of one ligand (ATP or substrate) influences the interaction of the chaperone with the other ligand (Figures 1A, S1A, and S1B) and, hence, require the presence of both ligands. Our methyl-TROSY data on the ATP/substrate-bound state of DnaK (Figure 2C) show that it is more similar to undocked (ADP-bound) DnaK than to the ATP-bound state, indicating that substrate binding induces domain undocking. Note in particular the lack of significant chemical shift perturbations in the SBD resonances relative to those of the substrate-bound isolated SBD (green in Figure 2C), including residues located on the interdomain interface. However, importantly, there are small but significant chemical shift differences between NBD resonances of the full-length ATP/substrate-bound DnaK and those of the isolated NBD (in the ATP-bound state) (see arrows in Figure 2C). It is instructive to compare the NBD in ATP/substrate-bound DnaK to previously characterized ATP-bound conformations of isolated NBDs that retain the conserved hydrophobic interdomain linker (DnaK(1-392)) or not (DnaK(1-388)) (Zhuravleva and Gierasch, 2011) (Figure 4A). Resonances from the NBD of ATP/substrate-bound DnaK fall between those of DnaK(1-392) and DnaK(1-388). Based on our previous results, the chemical shift differences between these two constructs are a result of conformational changes in the NBD attributable to binding of the interdomain linker. To directly test the involvement of the linker in ATP/substrate-bound DnaK, we carried out chemical shift perturbation analysis of ATPγS-bound DnaK(1-552) (which populates a conformational ensemble similar to that populated by ATP/substrate-bound full-length DnaK [see below]) using a "soft" mutation of one of the conserved hydrophobic residues in the linker (L390V). The resulting pattern of chemical shift changes revealed that the linker in ATP/substrate-bound DnaK interacts with the β strand of subdomain IIB (Figures 4B and S4A)—the same linker-binding site that was previously found for the isolated NBD (Zhuravleva and Gierasch, 2011). Additionally, we mutated three consecutive conserved hydrophobic linker residues (^{389}VLL^{391} to ^{389}DDD^{391}) to explore in greater depth the role of the linker in shifting the conformation of the undocked (ADP-bound) state of DnaK to its ATP/substrate-bound DnaK form. This mutation abolished the similarity of shifts for ATP/substrate-bound DnaK NBD resonances to those of ATP-bound DnaK(1-392), and the peaks now overlay on those of ATP-bound DnaK(1-388) (Figure 4C), indicating complete linker unbinding.

Based on these results, we conclude that the interdomain linker binds to the NBD in ATP/substrate-bound DnaK, whereas the SBD has undocked from the NBD. However, several lines of evidence make it clear that both the linker-bound and linker-unbound conformations are significantly populated in ATP/substrate-bound DnaK. First, intensities of the unbound linker resonances are reduced in ATP/substrate-bound DnaK relative to apo-DnaK (domain undocked, linker unbound), but the resonances remain, arguing that the linker is unbound in a fraction of the population and bound in the rest (Figures S4B and S4C). Second, the NBD chemical shifts in ATP/substrate-bound DnaK lie midway between the linker-unbound (DnaK(1-388)) and linker-bound (DnaK(1-392)) conformations (Figure 4A), which argues for a dynamic equilibrium between states with bound and unbound linker. Third, dynamic equilibration between linker-bound and linker-unbound states is also consistent with the observed overall decrease in peak intensities (more than 3-fold for most residues as compared with the apo, domain-undocked state) and line broadening in amide spectra of ATP/substrate-bound DnaK (Figure S2D).

The simultaneous action of ATP, which stabilizes linker binding to the NBD and domain docking, and substrate, which favors domain undocking and stabilizes the β-SBD-α-helical lid interaction, subjects DnaK to two opposing driving forces. The result is an ensemble of fluctuating, interconverting domain-undocked conformations, with a fraction linker bound and a fraction linker unbound, in equilibrium with the domain-docked state (Figure 4D). The properties of this ensemble account for the allosteric functions of DnaK: enhanced NBD ATPase activity upon substrate binding, and rapid substrate association/dissociation upon ATP binding. ATPase activation upon substrate binding is explained by the action of linker binding on the NBD in the absence of domain docking, which is sufficient to activate NBD ATPase activity to an extent comparable to activation by substrate binding (Swain et al., 2007; Vogel et al., 2006).

A "Tug-of-War" between Two Orthogonal Interfaces Explains Modulation of Hsp70 Allosteric Activity by Ligands, Mutations, and Evolutionary Variation

The two orthogonal interdomain sets of interactions in DnaK, the NBD-β-SBD interface, and the β-SBD-α-helical lid interface emerge as "tunable" elements that shape the allosteric landscape. Understanding the competitive energetic linkage of these interfaces provides a framework to explain several previous observations. For example, mutations that destabilize the NBD-β-SBD interface or stabilize the β-SBD-α-helical lid interface will decouple ATPase activation and substrate binding. Such interface variants will have significantly enhanced basal ATPase activity, and substrate binding will result in a minimal increase in the ATPase rate. As a specific example, the allosterically defective mutation K414I was identified in our lab (Montgomery et al., 1999); this residue substitution destabilizes the NBD-β-SBD interface as expected from the Hsp110-based model for the ATP-bound DnaK conformation, resulting in significant domain disengagement even without substrate, consistent with its red-shifted W102 fluorescence. Because of the weakening of the NBD-β-SBD interface, DnaK molecules harboring the K414I mutation (Figure 5A) populate the allosterically active, undocked, linker-bound DnaK conformation (Figure 5B, middle), which explains their enhanced basal ATPase activity. As would be predicted by this analysis of opposing energetic balances, perturbations of the NBD-β-SBD interface can also result in an opposite effect: the L390V mutation (Figure 5A) significantly stabilizes the docked state even in the presence of substrate (Figure 5C).

The nucleotide analog ATPγS does not mediate the same allosteric activities as the native ligand ATP (Theyssen et al., 1996). We now understand that ATPγS cannot shift the NBD fully to the conformation that forms a stable NBD-β-SBD interface

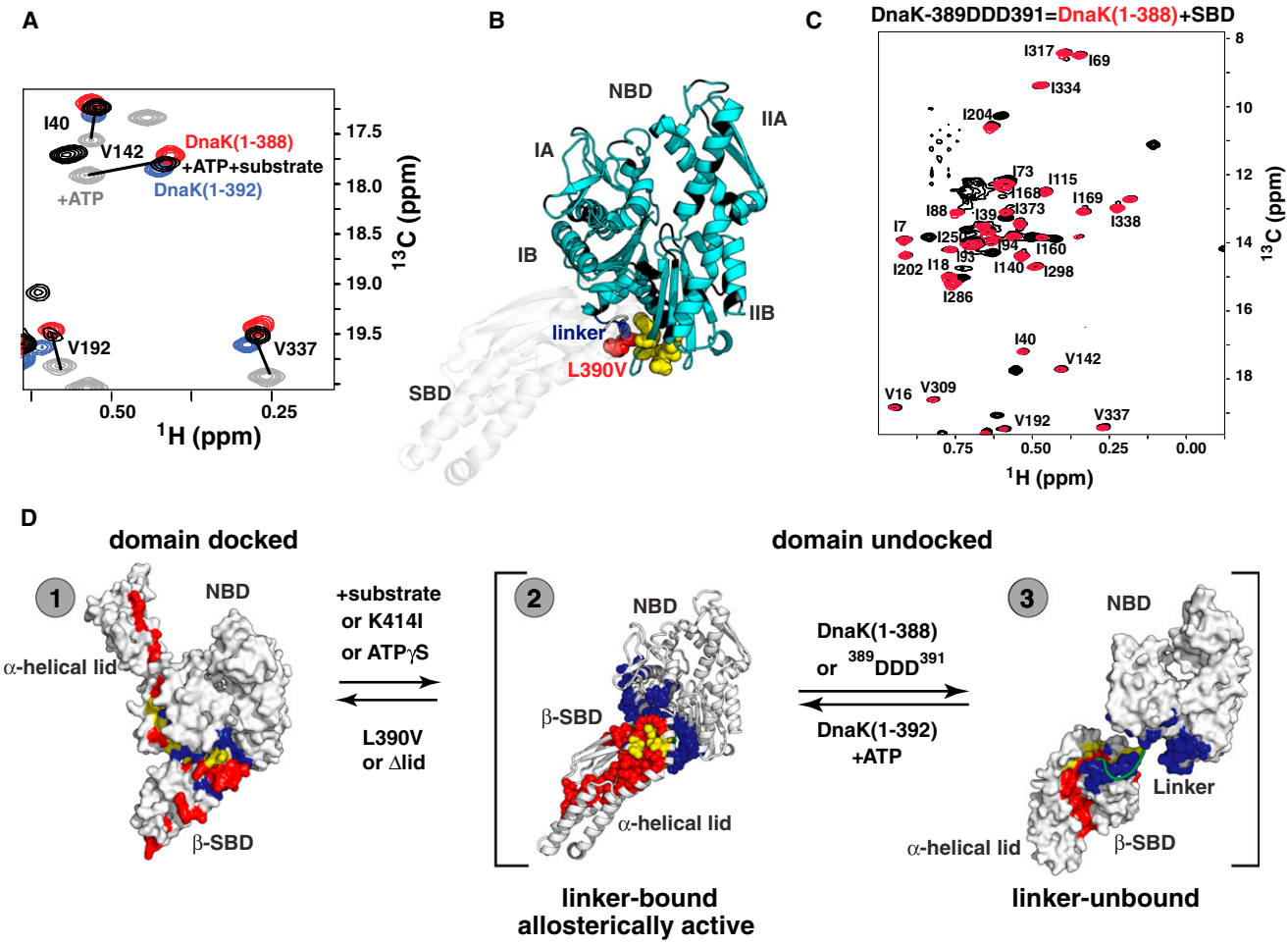

Figure 4. The Allosterically Active DnaK Intermediate

(A) Ligand-driven changes in the DnaK conformational ensemble are shown. Blowup of a representative region of methyl-TROSY spectra of ATP-bound DnaK in the absence of substrate (gray, the domain-docked state) and with substrate (black, the domain-undocked ensemble of linker-bound and -unbound conformations), overlaid on spectra of the isolated NBD, with linker (DnaK(1-392)) (blue, the linker-bound conformation) or without linker (DnaK(1-388)) (red, the linker-unbound, domain undocked conformation). Similar results were obtained for wild-type DnaK without the T199A mutation (see Figure S4).

(B) Linker-binding site on the NBD: residues that display significant chemical shift differences (more than 0.03 and 0.3 ppm for ^{1}HN and ^{15}N atoms, respectively) between the NBD of ATPγS-bound DnaK(1-552) (which samples both linker-bound and linker-unbound domain-undocked conformations) and its "soft" mutant L390V are shown in yellow on the modeled structure of the allosterically active conformation. To schematically model this conformation, the SBD of Hsp110-based homology model was replaced by the SBD from the ADP-bound DnaK (PDB 2kho) (see also Figure S4).

(C) The isoleucine region of the methyl-TROSY spectrum of the two-domain allosterically defective ^{389}DDD^{391} DnaK(1-605) bound to ATP and substrate (black) showing near-perfect overlap with spectra of the individual, nonlinker-bound NBD, DnaK(1-388) (red).

(D) Schematic illustration of two coupled conformational transitions in DnaK: (1) between the domain-docked conformation and the domain-undocked ensemble (corresponding to a transition between gray [ATP-bound] and black [ATP/substrate-bound] peaks on left); and (2) between linker-bound and -unbound conformations (corresponding to a transition between NBD plus linker [blue] and NBD only [red] peaks in A). Note in full-length DnaK that this transition is fast on the NMR timescale and that black peaks on the left correspond to the dynamic domain-undocked ensemble of these two conformations. Interdomain interfaces are colored as in Figure 3D.

(Figure 5B, bottom). Thus, ATPγS fails to stabilize the domain-docked conformation and results in significant domain disengagement. Remarkably, ATPγS binding does not perturb linker interaction with the NBD but rather results in small changes to the interdomain interface (Zhuravleva and Gierasch, 2011) that perturb domain docking.

Modulating the strength of interactions between the β-SBD and the α-helical lid should also remodel the allosteric landscape in a way that is explained by the dueling interfaces. We compared amide-TROSY spectra of full-length DnaK and its C-terminally truncated construct DnaK(1-552), which lacks the helical bundle of the α-helical lid (Figure 5A) and as a result, has substantially less stable secondary structure in helix B (Swain et al., 2006), leading to a weaker β-SBD-α-helical lid interaction. In the absence of substrate, this C-terminal truncation does not affect the docked, ATP-bound state, reflected in the similar basal ATPase activities of the full-length DnaK and DnaK(1-552) (Swain et al., 2006). But these truncated variants

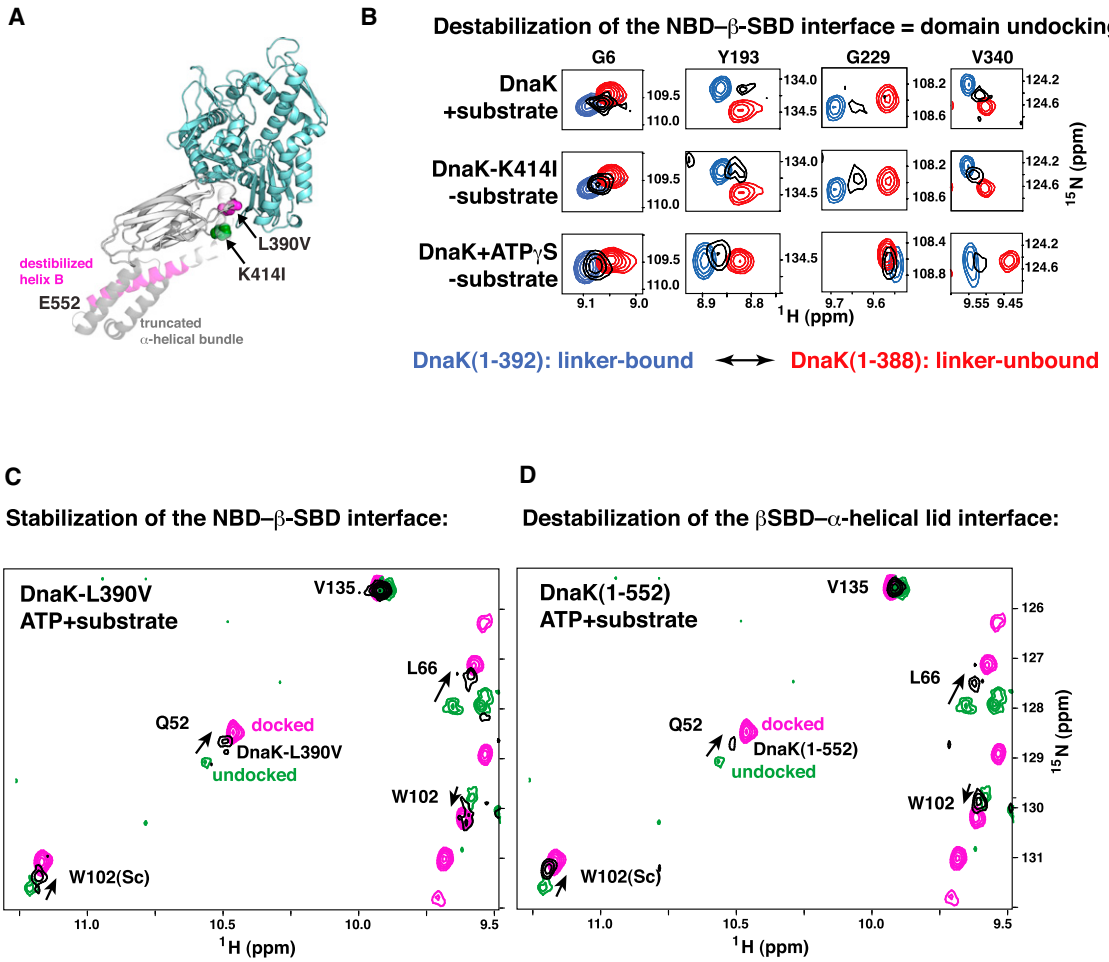

Figure 5. The Impact of Competition between the NBD-β-SBD and β-SBD-α-Helical Lid Interfaces on the Hsp70 Allosteric Landscape

(A) DnaK sequence modifications that result in perturbations in its conformational ensemble are mapped onto the modeled structure of the allosterically active conformation (modeled as for Figure 4): L390V and C-terminal truncations, which favor domain docking, are shown in magenta; K414I, which favors domain undocking, is shown in green.

(B) Destabilization of the NBD-β-SBD interface results in domain undocking even in the absence of substrate. Blowup of the amide-TROSY spectra of DnaK(1-392) (blue, representing the NBD linker-bound state) and DnaK(1-388) (red, representing the NBD linker-unbound state) overlaid on the spectra of two-domain DnaK under conditions that stabilize domain undocking, either upon substrate binding to the ATP-bound DnaK(1-605) (top panels) or upon perturbation of the NBD-β-SBD interface, viz ATP-bound DnaK(1-552)K414I (middle panels), or ATPγS-bound DnaK(1-552) (bottom panels). Resonances shown (Gly6, Tyr193, Gly229, and V340) report on long-range conformational changes in the nucleotide-binding site upon linker binding to the NBD (see Extended Experimental Procedures). The spectra of the isolated NBD constructs are with the corresponding nucleotide bound (ATP, top and middle panels) or ATPγS bound (bottom panels).

(C) Stabilization of the NBD-β-SBD interface in DnaK(1-605)L390V or (D) destabilization of the β-SBD-α-helical lid interaction in DnaK(1-552) favors the domain-docked conformation even in the presence of substrate. A representative region of the amide-TROSY spectra of the ATP-bound state of DnaK(1-552) (magenta; the domain-docked conformation) and ATP/substrate-bound DnaK(1-605) (green; the domain-undocked ensemble of linker-bound and linker-unbound conformations) overlaid with spectra of DnaK(1-605)L390V (C) and DnaK(1-552) (D), shown in black. Consistent with previous biochemical studies by Kumar et al. (2011) and Swain et al. (2007), neither the L390V mutation on the NBD-β-SBD interface nor disruption of the β-SBD-α-helical lid interface in DnaK(1-552) affects the ATP-bound conformation in the absence of substrate.

display a reduction in the degree to which the substrate shifts the equilibrium toward the domain-undocked ensemble (Figure 5D). This interpretation fully explains why DnaK(1-552) displays a reduced substrate-activated ATPase rate (about two times lower than that of full-length DnaK) (Swain et al., 2006).

Given the functional significance of the NBD-β-SBD and β-SBD-α-helical lid interfaces, we anticipated high conservation of residues located on these interfaces and indeed found this to be true. The residues interacting across these interfaces are identical in 80% and 70% for the NBD-β-SBD and β-SBD-α-helical lid interfaces, respectively (Figure 6A), in a set of Hsp70s (see Experimental Procedure). In addition, statistical coupling analysis to reveal conservation of correlated variations found several linkages between these interfaces (Smock et al., 2010).

Despite their high conservation, Hsp70s display some amino acid substitutions on the interdomain interfaces (Figure 6B). To

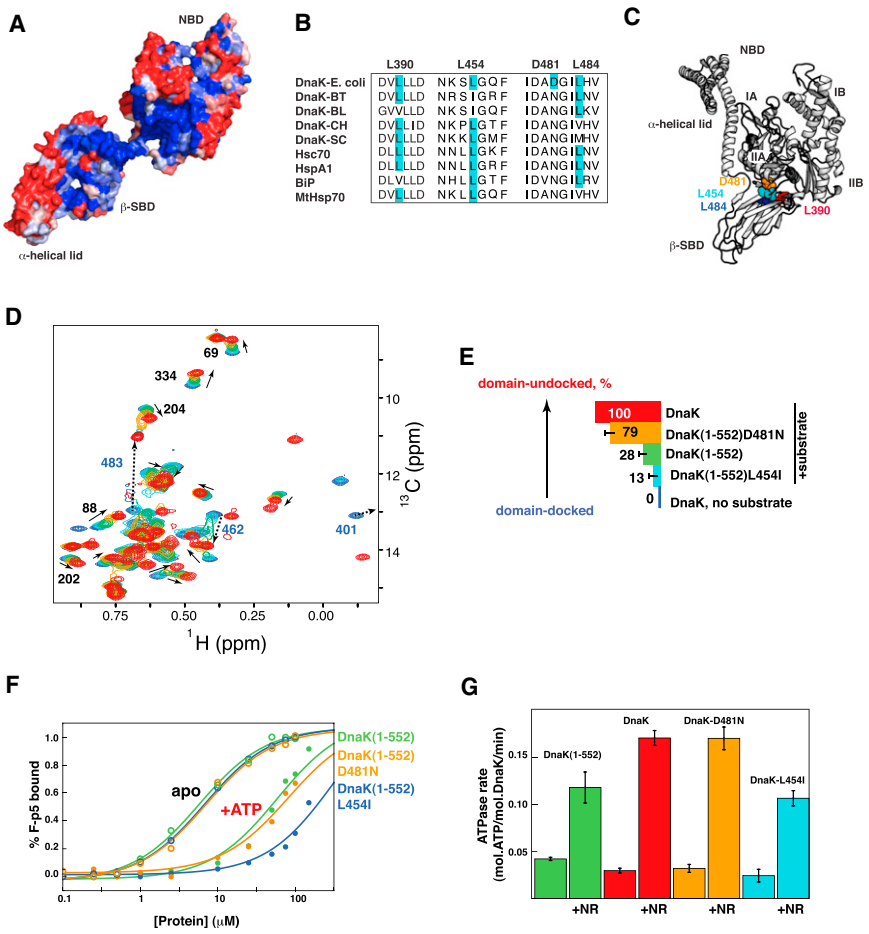

Figure 6. Evolutionary Variation at the NBD-β-SBD and β-SBD-α-Helical Lid Interfaces Modulates the Hsp70 Allosteric Landscape

(A–C) Sequence conservation and diversity at the NBD-β-SBD interdomain interface in the Hsp70 family. (A) Sequence conservation between different Hsp70 family members colored from blue for fully conserved residues to red for residues with no conservations (see Experimental Procedures) shown on the structure of ADP-bound DnaK state (PDB 2kho). (B) Multiple sequence alignment (ClustalW) of DnaKs from *E. coli*, *Bacteroides thetaiotaomicron VPI-5482* (BT), *Bifidobacterium longum NCC2705* (BL), *Cytophaga hutchinsonii* (CH), and *Streptomyces coelicolor A3(2)* (SC), and four human Hsp70s (Hsc70, HspA1, endoplasmic reticulum-BiP, and mitochondrial-MtHsp70). (C) Observed amino acid substitutions identified in (B) are shown on the Hsp110-based homology model.

(D) The isoleucine region of methyl-TROSY spectra of ATP-bound full-length DnaK in the absence of substrate (blue, corresponding to the docked state) and with substrate (red, corresponding to the domain-undocked ensemble, which is comprised of a mixture of linker-bound and linker-unbound conformations). Overlaid on these are variants that partition between docked and undocked states, including ATP/substrate-bound DnaK(1-552) (green), ATP/substrate-bound DnaK(1-552)L454I (light blue), and ATP/substrate-bound DnaK(1-552)D481N (orange). ATP/substrate-bound DnaK(1-552)L484I shows very similar results to L454I (Table S1). All experiments were performed at saturating substrate concentrations (2 mM of NR peptide) (see also Figure S5).

(E) Histogram showing the degree of substrate-induced domain undocking for individual constructs, colored as in (C and D). For each DnaK variant, the degree of domain undocking was estimated as described in the Experimental Procedures.

(F and G) Tuning of DnaK functionality. (F) Equilibrium binding of a fluorescently labeled peptide substrate to DnaK(1-552) (green) and its variants L454I (cyan) and D481N (orange) in the presence of ADP (open circles) and ATP (filled circles). K_D values are 5.7 ± 1.0 μM (60 ± 20 μM), 6.9 ± 1.0 μM (80 ± 20 μM), and 6.8 ± 1.0 μM (300 ± 70 μM) for the ADP-(ATP-)bound state of DnaK(1-552), DnaK(1-552)-D481N, and DnaK(1-552)-L454I, respectively (see Extended Experimental Procedures). (G) Stimulation of the ATPase activity of wild-type DnaK (red) and its variants DnaK-L454I (cyan), DnaK-D481N (orange), and DnaK(1-552) (green) by 200 μM NR peptide. Error bars show SDs from the means for three replicate experiments (see Figure S5I and Extended Experimental Procedures).

explore whether evolutionarily selected substitutions on the NBD-β-SBD interfaces affect Hsp70 conformational equilibrium and consequently functional properties, we tested several DnaK(1-552) variants based on known amino acid variations on the interdomain interfaces: L454I, D481N, and L484I (Figures 6B and 6C). Although *E. coli* DnaK can tolerate these mutations in vivo (Figure S5A), these amino acid substitutions significantly affect the DnaK conformational ensemble by changing the degree to which substrate in the presence of ATP shifts the equilibrium between domain-docked and domain-undocked conformations (Figures 6D, 6E, and S5F–S5H; Table S1). Upon substrate binding, the tension and balances among the NBD, β-SBD, and α-helical lid couplings result in a highly tunable Hsp70 conformational ensemble, for which even minor changes on the interdomain interfaces (such as the L390V, L454I, D481N, and L484I substitutions; Figure 6C) significantly affect the conformational equilibrium and, consequently, function, because stabilization of the docked conformation results in decrease of substrate affinity and ATPase activity (Figures 6F and 6G). In turn, substrate-binding affinity affords another tunable energetic contribution because higher affinity substrates shift the equilibrium toward the allosterically active state (Figures S5C, S5F, and S5G).

DISCUSSION

This study has provided insights into the fundamental mechanism of allostery of a paradigmatic Hsp70, DnaK (Figures 7 and S6). We find that the Hsp70 allosteric landscape comprises three distinct protein conformations (Figure 7A): undocked (ADP-bound) and docked (ATP-bound) "endpoint" states, and an intermediate, the allosterically active, domain-dissociated linker-bound conformation, that is partially populated in the presence of ATP and substrate. Each conformation is characterized by different arrangements of Hsp70 allosteric structural elements (NBD, β-SBD, α-helical lid), whereas two flexible

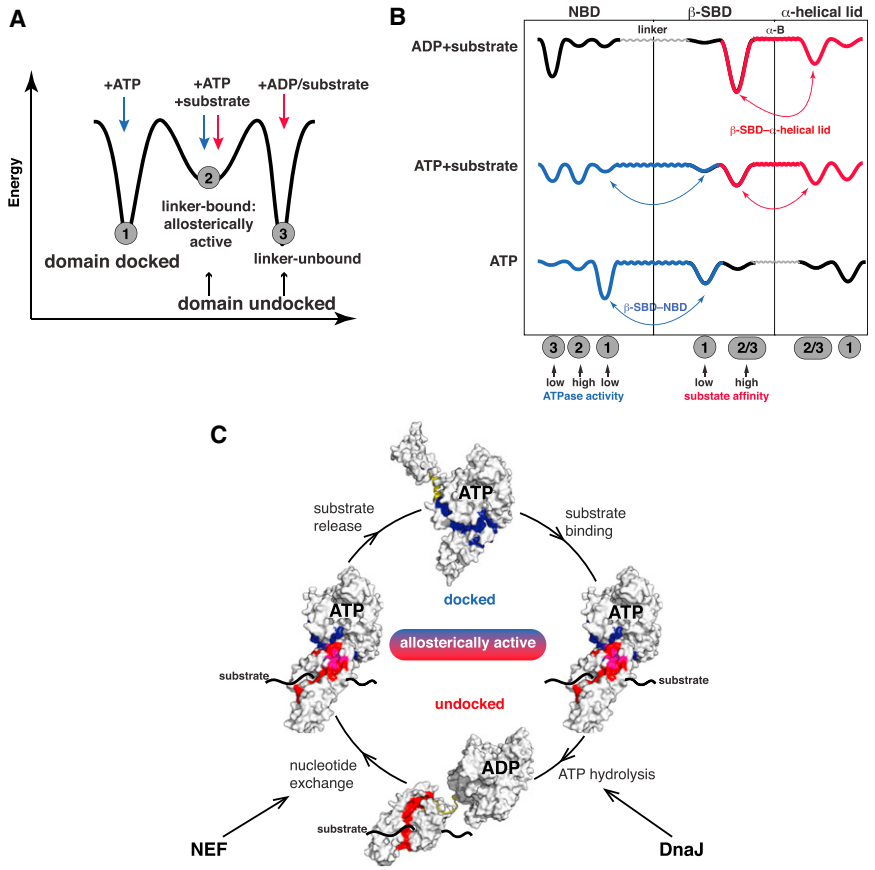

Figure 7. Mechanism of Hsp70 Allostery

(A and B) Schematic illustration of Hsp70 allosteric landscapes showing how the allosterically active state serves as an intermediate between the two "endpoint" states (A) and (B) how thermodynamic coupling of Hsp70 domains determines the conformations the protein populates along its allosteric cycle (see also Figures 4D and S6): binding of ADP and substrate favors interactions between the β-SBD and α-helical lid (red, in the domain-undocked conformation); ATP-induced linker binding to the NBD favors NBD-SBD docking (blue, in the domain-docked conformation). In the presence of both ATP and substrate, an interdomain energetic "tug-of-war" results in a highly dynamic and tunable conformational ensemble. The interdomain linker and helix B provide flexible and ligand-adjustable connections among the NBD, the β-SBD, and the α-helical lid. (C) Illustration of the roles of energetic interdomain coupling and "tunability" in the allosteric cycle. The interfaces between the NBD and the β-SBD and between the β-SBD and the α-helical lid are shown in blue and red, respectively, and in magenta are shown residues that participate in both interfaces. These interfaces define the thermodynamics and kinetics of the allosteric cycle and can be modulated by either intrinsic (sequence changes) or extrinsic (binding to nucleotide, substrates, cochaperones) factors.

regions—the interdomain linker and helix B of the helical lid—provide adjustable coupling connections between these units and create tunable interfaces between the structural elements (Figure 7B). This "Lego"-like architecture creates a set of thermodynamic linkages that provide an explanation for the fundamental mystery of Hsp70 allostery: how events at each of the two domains can influence the other domain.

Allostery in Hsp70s is achieved because binding of nucleotide and substrate ligands is thermodynamically linked so as to control the conformations of individual domains. In order for this allosteric machine to function, each separate domain must possess the capacity to sample (at least) two distinct conformations (Figure 7B). The result of linkages between domains is a state endowed with the properties required for active allostery (Csermely et al., 2010; del Sol et al., 2009; Smock and Gierasch, 2009): ability to "breathe" and sample multiple local conformations, including one with a catalytically active array of nucleotide ligands, and one with an unlidded, disturbed substrate-binding site, which should have fast and reversible substrate-binding/release. In the allosteric cycle of an Hsp70 depicted in Figure 7C, this state corresponds to the obligatory intermediate between the two endpoint ADP- and ATP-bound states. For the isolated NBD, the binding of ATP perturbs the intradomain conformation so as to favor linker binding and high ATPase activity (Bhattacharya et al., 2009; Revington et al., 2004; Zhuravleva and Gierasch, 2011). In full-length DnaK, this ATP-induced linker binding transmits a signal to the SBD via stabilizing interactions between the NBD and SBD. Note that only minor changes in reorientations of NBD subdomains drastically affect ATPase activity of the protein (Zhuravleva and Gierasch, 2011), which explains how interactions between the linker and the NBD (in the allosterically active, domain-undocked conformation) and between the NBD and the SBD (in the docked conformation) significantly affect ATPase activity. Binding of substrate is coupled to these NBD conformational changes because of its direct stabilizing effect on the β-SBD-α-helical lid interface and indirect destabilizing effect on the NBD-β-SBD interface. For the SBD, only one of its conformations has been described at atomic resolution. However, our results clearly demonstrate that domain docking stabilizes a very different unlidded β-SBD conformation that we know has a markedly reduced capacity to bind substrates.

The delicate balance among conformational states created by thermodynamic coupling of opposing energetic contributions leads to exquisite "tunability" of the Hsp70 system (Figure 6E). Each "endpoint" Hsp70 state is stabilized by only one major intrinsic interaction (Figure 7B): either the β-SBD-α-helical lid interaction in the undocked state (in the presence of ADP and substrate), or the NBD-β-SBD interaction in the docked (ATP-bound) state, whereas both interactions contribute to the allosterically active (ATP- and substrate-bound) conformation. Consequently, even minor perturbations of these interfaces result in redistributions in the Hsp70 conformational ensemble and (through resulting ATPase activity and substrate affinity)

define kinetics and thermodynamics of the Hsp70 allosteric cycle. Thus, the conformational distribution underlying the Hsp70 allosteric cycle can be readily shifted by either internal (sequence changes) or external factors (binding to cochaperones, other chaperones, and different substrates).

The energetic tug-of-war in Hsp70s between intradomain interactions and interdomain interfaces provides an explanation for a number of previous observations, including a marked decrease in substrate affinity upon perturbation of the β-SBD-α-helical lid interaction (Fernández-Sáiz et al., 2006; Moro et al., 2004) and the fact that ATPase stimulation is proportional to substrate affinity (Mayer et al., 2000). Alterations in substrate-binding affinity or kinetics clearly alter the allosteric reaction propensities. As a result, the behavior of the Hsp70 can be tuned to individual substrates, depending on their folding and aggregation properties, or on the physiological situation. DnaK is a "hub" among chaperone networks and forms complexes with at least 700 substrates (Calloni et al., 2012): its tunability enables it to perform its allosteric cycle differently, depending on these extrinsic factors. Moreover, binding to a large substrate will significantly destabilize the interaction between the β-SBD and the α-helical lid (Schlecht et al., 2011), providing yet another way to affect the Hsp70 ensemble and result in substrate-dependent modulation of Hsp70 function.

Cochaperones serve as extrinsic contributors to the allosteric balancing act in Hsp70s. We speculate that cochaperone effects on Hsp70s will be clarified in terms of the balance of intra- and interdomain interactions. For example, shifting of the equilibrium between the linker-bound and linker-unbound conformations likely underlies the ability of the DnaJ class of cochaperones to enhance Hsp70 ATPase activities (Jiang et al., 2007). A recently discovered dynamic interface between DnaJ and DnaK (the residue 206 to residue 221 of the NBD) (Ahmad et al., 2011) overlaps with the NBD-SBD interdomain interfaces and provides another means to regulate Hsp70 ATPase activity.

The "tunability" of the Hsp70 system offers an explanation for the striking functional diversity in the Hsp70 family (Kampinga and Craig, 2010; Sharma and Masison, 2011). Evolutionary tuning can occur via sequence changes at the key coupling interfaces. As illustrated above (Figure 6), even single conservative amino acid changes shift the equilibrium among docked, undocked (linker-unbound), and allosterically active (linker-bound) states and thus "tune" conformational distributions to adjust kinetics and thermodynamic of the allosteric cycle to specific substrates, environment, and function in different Hsp70 members. It will be of great interest to further explore the impact of sequence variations in these key interfaces among the Hsp70 family.

Taken together, our results provide insights into the mechanism of Hsp70 allostery that explain many previous experimental observations, elucidate the basis of the striking functional diversity within the Hsp70 family, and reveal "tunable" allosteric segments in Hsp70, which comprise potential binding sites for Hsp70 cochaperones. The insights into "tunability" also provide a basis for design of small allosteric modulators of Hsp70 function, which are shown to have the great potential for therapeutic targeting of the Hsp70 system (Chang et al., 2011; Rousaki et al., 2011). Our data on Hsp70s also have implications more broadly because allostery in other systems is likely to exploit analogous ligand-modulated changes in thermodynamic linkages between protein domains and allosteric interfaces. From an evolutionary standpoint, it is clear from the Hsp70 system that linking conformational equilibria within domains via interdomain interfaces is a blueprint to create allosteric signaling in multidomain protein systems. Indeed, recent work from the Ranganathan lab has illustrated successful creation of allosteric signaling by combining otherwise nonallosteric proteins (Halabi et al., 2009). We believe that the same mechanistic principles harnessed in the two-domain Hsp70s can also be extended as a general allosteric mechanism for other multidomain protein systems and for protein complexes with coupled allosteric functions.

EXPERIMENTAL PROCEDURES

Construct Design and NMR Experiments

We designed three C-terminally truncated constructs each including the T199A mutation (Figure 1D), including DnaK(1-507), which comprises the NBD and β-SBD only; DnaK(1-552), containing the NBD and β-SBD plus helices A and B of the α-helical lid; and DnaK(1-605), including the NBD, β-SBD, and the whole α-helical lid. In the C-terminally truncated constructs, we incorporated L542Y and L543E mutations to disfavor self-binding (the helical lid back to the substrate-binding site) and ensure the same allosteric landscape as in full-length DnaK (Swain et al., 2006). Expression and purification of uniformly and ligated ^{2}H-,^{13}C-,^{15}N-labeled, and ^{2}H-Methyl-^{13}CH$_3$-labeled samples were performed according to published methods (Tugarinov et al., 2006; Zhuravleva and Gierasch, 2011; Clerico et al., 2010). NMR samples contained 300–500 μM (for backbone NMR analysis) or ~50–100 μM (for methyl NMR) of the protein, 10 mM of potassium phosphate (pH 7.0), and if needed, 5 mM of appropriate nucleotide, 5 mM $MgCl_2$, 2 mM NR (NRLLLTG) peptide as a substrate (saturating for all constructs; Figure S5B). All NMR spectra in this study were obtained at 26°C on a 600 MHz Bruker Avance spectrometer using a TXI cryoprobe or 700 MHz Varian NMR system equipped with a cryogenically cooled triple-resonance probe. Spectra were processed using NMRPipe (Delaglio et al., 1995) and analyzed using Cara (Keller, 2004). Backbone assignments for the nucleotide-free and ATP-bound states of DnaK(1-388) and DnaK(1-392) and peptide-bound and -free SBD(387-552) were transferred from previous assignments (Swain et al., 2006; Zhuravleva and Gierasch, 2011) using TROSY-modified versions of HNCO and HNCA experiments (Weigelt, 1998). Methyl assignments of ^{1}H$^{\delta}$ and ^{13}C$^{\delta}$ of isoleucines were facilitated using the 3D HMCMCA and HMCMCB experiments (Tugarinov and Kay, 2003). To assign backbone spectra of ATP-bound DnaK, we applied a "divide-and-conquer" strategy (Gelis et al., 2007; Ruschak and Kay, 2010), in which fragments of a protein are assigned, followed by the transfer of this assignment to the bigger constructs. The (^{1}H$^{\delta}$,^{13}C$^{\delta}$) methyl assignments for nonoverlapping NBD peaks were transferred from the assignments of the isolated NBD. The partial assignments of SBD peaks were obtained using single-point mutagenesis. For more details, see Extended Experimental Procedures.

Chemical Shift Analysis

To identify the residues that experience large structural and/or dynamic perturbations between different constructs, we performed a pairwise comparison of chemical shifts. For each residue, we calculated a total chemical shift difference: $\Delta\delta = \sqrt{((\Delta\delta_H)^2 + (0.154\Delta\delta_N)^2 + (0.341\Delta\delta_{CO})^2)}$, where $\Delta\delta_H$, $\Delta\delta_N$, and $\Delta\delta_{CO}$ are ^{1}HN, ^{15}N, and ^{13}CO chemical shift differences, respectively, between two constructs. Chemical shift differences were considered as significant if any of $\Delta\delta_H$, $\Delta\delta_N$, or $\Delta\delta_{CO}$ was two-fold larger than the corresponding chemical shift errors, i.e., 0.08, 0.8, and 0.5 ppm for ^{1}HN, ^{15}N, and ^{13}CO atoms, respectively.

To identify interdomain interfaces, we constructed several "soft" single-point β-SBD and α-helical lid mutations on the interdomain interfaces predicted from the Hsp110-based model: L390V, L454I, D481N, E511D, and

M515I. Residues with backbone chemical shift differences, $\Delta\delta_{HN}$ >0.03 ppm and/or $\Delta\delta_N$ >0.3 ppm (for the L390V, L454I, D481N, E511D DnaK constructs), or methyl chemical shift, $\Delta\delta_H$ >0.01 ppm and/or $\Delta\delta_C$ >0.1 ppm (for the DnaK(1-552)-M515I) between DnaK(1-552) and a corresponding construct were considered to be affected by a given mutation.

To obtain estimates of the degree of domain undocking for different DnaK constructs in the ATP/substrate-bound state, we used methyl chemical shifts of six NBD isoleucine residues (I40, I69, I88, I202, I204, and I334), which have well-resolved methyl peaks in NMR spectra of different constructs (Figure 6D). For these calculations, we assumed that for these residues, the domain-docking/undocking transition is fast on the NMR timescale, and the observed peak position is therefore a population-weighted average of the chemical shifts of the domain-docked conformation (ATP-bound DnaK) and domain-undocked ensemble (ATP/substrate-bound DnaK). Further details are given in Table S1.

Functional DnaK Assays

ATPase and substrate-binding anisotropy assays were measured as previously described by Chang et al. (2008) and Montgomery et al. (1999), respectively. For more details see Extended Experimental Procedures.

Homology Models and Definition of Interdomain Interfaces

We used the Hsp110-based homology model for DnaK developed previously by Smock et al. (2010) (coordinates are available upon request). For the undocked (Protein Data Bank ID code [PDB] 2kho) and docked (the Hsp110-based homology model) conformations, a residue was defined to reside on an interdomain interface if any of its atoms were located within 5 Å from any atoms belonging to the other allosteric units (the NBD, β-SBD, α-helical lid, or interdomain linker). To model the allosterically active (domain-undocked/linker-bound) conformation, the SBD was removed from the structure, and the SBD from the ADP-bound DnaK (PDB 2kho) was aligned on the β-SBD of the Hsp110-based homology model.

Evolutionary Conservation in the Hsp70 Family

Sequence conservation among different Hsp70 family members was estimated using the ConSurf Server (http://consurf.tau.ac.il; Glaser et al., 2003), a multiple sequence alignment was built using ClustalW, and the homolog search algorithm used was CS-BLAST, with the minimal identity for homologs at 60%. A total of 150 homologs with the lowest E values were used for analysis. Residue varieties for the highly conserved residues 390, 454, 481, and 484 were (L and V), (interM,I, and L), (N and D), and (M, I, L, and V), respectively.

SUPPLEMENTAL INFORMATION

Supplemental Information includes Extended Experimental Procedures, six figures, and one table and can be found with this article online at http://dx.doi.org/10.1016/j.cell.2012.11.002.

ACKNOWLEDGMENTS

This work was supported by NIH grant GM027616. We thank Fabian Romano and Alejandro Heuck for assistance with the time-resolved fluorescence measurements.

Received: April 23, 2012
Revised: August 10, 2012
Accepted: October 23, 2012
Published: December 6, 2012

REFERENCES

Ahmad, A., Bhattacharya, A., McDonald, R.A., Cordes, M., Ellington, B., Bertelsen, E.B., and Zuiderweg, E.R.P. (2011). Heat shock protein 70 kDa chaperone/DnaJ cochaperone complex employs an unusual dynamic interface. Proc. Natl. Acad. Sci. USA *108*, 18966–18971.

Bertelsen, E.B., Chang, L., Gestwicki, J.E., and Zuiderweg, E.R.P. (2009). Solution conformation of wild-type *E. coli* Hsp70 (DnaK) chaperone complexed with ADP and substrate. Proc. Natl. Acad. Sci. USA *106*, 8471–8476.

Bhattacharya, A., Kurochkin, A.V., Yip, G.N.B., Zhang, Y., Bertelsen, E.B., and Zuiderweg, E.R.P. (2009). Allostery in Hsp70 chaperones is transduced by subdomain rotations. J. Mol. Biol. *388*, 475–490.

Buchberger, A., Theyssen, H., Schröder, H., McCarty, J.S., Virgallita, G., Milkereit, P., Reinstein, J., and Bukau, B. (1995). Nucleotide-induced conformational changes in the ATPase and substrate binding domains of the DnaK chaperone provide evidence for interdomain communication. J. Biol. Chem. *270*, 16903–16910.

Bukau, B., and Walker, G.C. (1990). Mutations altering heat shock specific subunit of RNA polymerase suppress major cellular defects of *E. coli* mutants lacking the DnaK chaperone. EMBO J. *9*, 4027–4036.

Calloni, G., Chen, T., Schermann, S.M., Chang, H.C., Genevaux, P., Agostini, F., Tartaglia, G.G., Hayer-Hartl, M., and Hartl, F.U. (2012). DnaK functions as a central hub in the *E. coli* chaperone network. Cell Rep. *1*, 251–264.

Chang, L., Bertelsen, E.B., Wisén, S., Larsen, E.M., Zuiderweg, E.R., and Gestwicki, J.E. (2008). High-throughput screen for small molecules that modulate the ATPase activity of the molecular chaperone DnaK. Anal. Biochem. *372*, 167–176.

Chang, L., Miyata, Y., Ung, P.M.U., Bertelsen, E.B., McQuade, T.J., Carlson, H.A., Zuiderweg, E.R.P., and Gestwicki, J.E. (2011). Chemical screens against a reconstituted multiprotein complex: myricetin blocks DnaJ regulation of DnaK through an allosteric mechanism. Chem. Biol. *18*, 210–221.

Clerico, E.M., Zhuravleva, A., Smock, R.G., and Gierasch, L.M. (2010). Segmental isotopic labeling of the Hsp70 molecular chaperone DnaK using expressed protein ligation. Biopolymers *94*, 742–752.

Csermely, P., Palotai, R., and Nussinov, R. (2010). Induced fit, conformational selection and independent dynamic segments: an extended view of binding events. Trends Biochem. Sci. *35*, 539–546.

Delaglio, F., Grzesiek, S., Vuister, G.W., Zhu, G., Pfeifer, J., and Bax, A. (1995). NMRPipe: a multidimensional spectral processing system based on UNIX pipes. J. Biomol. NMR *6*, 277–293.

del Sol, A., Tsai, C.-J., Ma, B., and Nussinov, R. (2009). The origin of allosteric functional modulation: multiple pre-existing pathways. Structure *17*, 1042–1050.

Fernández-Sáiz, V., Moro, F., Arizmendi, J.M., Acebrón, S.P., and Muga, A. (2006). Ionic contacts at DnaK substrate binding domain involved in the allosteric regulation of lid dynamics. J. Biol. Chem. *281*, 7479–7488.

Flaherty, K.M., DeLuca-Flaherty, C., and McKay, D.B. (1990). Three-dimensional structure of the ATPase fragment of a 70K heat-shock cognate protein. Nature *346*, 623–628.

Gelis, I., Bonvin, A.M.J.J., Keramisanou, D., Koukaki, M., Gouridis, G., Karamanou, S., Economou, A., and Kalodimos, C.G. (2007). Structural basis for signal-sequence recognition by the translocase motor SecA as determined by NMR. Cell *131*, 756–769.

Glaser, F., Pupko, T., Paz, I., Bell, R.E., Bechor-Shental, D., Martz, E., and Ben-Tal, N. (2003). ConSurf: identification of functional regions in proteins by surface-mapping of phylogenetic information. Bioinformatics *19*, 163–164.

Halabi, N., Rivoire, O., Leibler, S., and Ranganathan, R. (2009). Protein sectors: evolutionary units of three-dimensional structure. Cell *138*, 774–786.

Hartl, F.U., Bracher, A., and Hayer-Hartl, M. (2011). Molecular chaperones in protein folding and proteostasis. Nature *475*, 324–332.

Jiang, J., Maes, E.G., Taylor, A.B., Wang, L., Hinck, A.P., Lafer, E.M., and Sousa, R. (2007). Structural basis of J cochaperone binding and regulation of Hsp70. Mol. Cell *28*, 422–433.

Kampinga, H.H., and Craig, E.A. (2010). The HSP70 chaperone machinery: J proteins as drivers of functional specificity. Nat. Rev. Mol. Cell Biol. *11*, 579–592.

Keller, R. (2004). Optimizing the process of nuclear magnetic resonance spectrum analysis and computer aided resonance assignment. PhD thesis, ETH, Zurich.

Kumar, D.P., Vorvis, C., Sarbeng, E.B., Cabra Ledesma, V.C., Willis, J.E., and Liu, Q. (2011). The four hydrophobic residues on the Hsp70 inter-domain linker have two distinct roles. J. Mol. Biol. *411*, 1099–1113.

Liu, Q., and Hendrickson, W.A. (2007). Insights into Hsp70 chaperone activity from a crystal structure of the yeast Hsp110 Sse1. Cell *131*, 106–120.

Manley, G., and Loria, J.P. (2012). NMR insights into protein allostery. Arch. Biochem. Biophys. *519*, 223–231.

Mapa, K., Sikor, M., Kudryavtsev, V., Waegemann, K., Kalinin, S., Seidel, C.A.M., Neupert, W., Lamb, D.C., and Mokranjac, D. (2010). The conformational dynamics of the mitochondrial Hsp70 chaperone. Mol. Cell *38*, 89–100.

Marcinowski, M., Höller, M., Feige, M.J., Baerend, D., Lamb, D.C., and Buchner, J. (2011). Substrate discrimination of the chaperone BiP by autonomous and cochaperone-regulated conformational transitions. Nat. Struct. Mol. Biol. *18*, 150–158.

Mayer, M.P., and Bukau, B. (2005). Hsp70 chaperones: cellular functions and molecular mechanism. Cell. Mol. Life Sci. *62*, 670–684.

Mayer, M.P., Schröder, H., Rüdiger, S., Paal, K., Laufen, T., and Bukau, B. (2000). Multistep mechanism of substrate binding determines chaperone activity of Hsp70. Nat. Struct. Biol. *7*, 586–593.

Mayer, M.P., Brehmer, D., Gässler, C.S., and Bukau, B. (2001). Hsp70 chaperone machines. Adv. Protein Chem. *59*, 1–44.

McCarty, J.S., and Walker, G.C. (1991). DnaK as a thermometer: threonine-199 is site of autophosphorylation and is critical for ATPase activity. Proc. Natl. Acad. Sci. USA *88*, 9513–9517.

Montgomery, D.L., Morimoto, R.I., and Gierasch, L.M. (1999). Mutations in the substrate binding domain of the *Escherichia coli* 70 kDa molecular chaperone, DnaK, which alter substrate affinity or interdomain coupling. J. Mol. Biol. *286*, 915–932.

Moro, F., Fernández, V., and Muga, A. (2003). Interdomain interaction through helices A and B of DnaK peptide binding domain. FEBS Lett. *533*, 119–123.

Moro, F., Fernández-Sáiz, V., and Muga, A. (2004). The lid subdomain of DnaK is required for the stabilization of the substrate-binding site. J. Biol. Chem. *279*, 19600–19606.

Revington, M., Holder, T.M., and Zuiderweg, E.R.P. (2004). NMR study of nucleotide-induced changes in the nucleotide binding domain of *Thermus thermophilus* Hsp70 chaperone DnaK: implications for the allosteric mechanism. J. Biol. Chem. *279*, 33958–33967.

Rist, W., Graf, C., Bukau, B., and Mayer, M.P. (2006). Amide hydrogen exchange reveals conformational changes in hsp70 chaperones important for allosteric regulation. J. Biol. Chem. *281*, 16493–16501.

Rousaki, A., Miyata, Y., Jinwal, U.K., Dickey, C.A., Gestwicki, J.E., and Zuiderweg, E.R.P. (2011). Allosteric drugs: the interaction of antitumor compound MKT-077 with human Hsp70 chaperones. J. Mol. Biol. *411*, 614–632.

Ruschak, A.M., and Kay, L.E. (2010). Methyl groups as probes of supramolecular structure, dynamics and function. J. Biomol. NMR *46*, 75–87.

Schlecht, R., Erbse, A.H., Bukau, B., and Mayer, M.P. (2011). Mechanics of Hsp70 chaperones enables differential interaction with client proteins. Nat. Struct. Mol. Biol. *18*, 345–351.

Sharma, D., and Masison, D.C. (2011). Single methyl group determines prion propagation and protein degradation activities of yeast heat shock protein (Hsp)-70 chaperones Ssa1p and Ssa2p. Proc. Natl. Acad. Sci. USA *108*, 13665–13670.

Smock, R.G., and Gierasch, L.M. (2009). Sending signals dynamically. Science *324*, 198–203.

Smock, R.G., Rivoire, O., Russ, W.P., Swain, J.F., Leibler, S., Ranganathan, R., and Gierasch, L.M. (2010). An interdomain sector mediating allostery in Hsp70 molecular chaperones. Mol. Syst. Biol. *6*, 414.

Swain, J.F., Schulz, E.G., and Gierasch, L.M. (2006). Direct comparison of a stable isolated Hsp70 substrate-binding domain in the empty and substrate-bound states. J. Biol. Chem. *281*, 1605–1611.

Swain, J.F., Dinler, G., Sivendran, R., Montgomery, D.L., Stotz, M., and Gierasch, L.M. (2007). Hsp70 chaperone ligands control domain association via an allosteric mechanism mediated by the interdomain linker. Mol. Cell *26*, 27–39.

Theyssen, H., Schuster, H.P., Packschies, L., Bukau, B., and Reinstein, J. (1996). The second step of ATP binding to DnaK induces peptide release. J. Mol. Biol. *263*, 657–670.

Tugarinov, V., and Kay, L.E. (2003). Ile, Leu, and Val methyl assignments of the 723-residue malate synthase G using a new labeling strategy and novel NMR methods. J. Am. Chem. Soc. *125*, 13868–13878.

Tugarinov, V., and Kay, L.E. (2005). Methyl groups as probes of structure and dynamics in NMR studies of high-molecular-weight proteins. ChemBioChem *6*, 1567–1577.

Tugarinov, V., Hwang, P.M., Ollerenshaw, J.E., and Kay, L.E. (2003). Cross-correlated relaxation enhanced 1H-13C NMR spectroscopy of methyl groups in very high molecular weight proteins and protein complexes. J. Am. Chem. Soc. *125*, 10420–10428.

Tugarinov, V., Kanelis, V., and Kay, L.E. (2006). Isotope labeling strategies for the study of high-molecular-weight proteins by solution NMR spectroscopy. Nat. Protoc. *1*, 749–754.

Tzeng, S.R., and Kalodimos, C.G. (2011). Protein dynamics and allostery: an NMR view. Curr. Opin. Struct. Biol. *21*, 62–67.

Vogel, M., Mayer, M.P., and Bukau, B. (2006). Allosteric regulation of Hsp70 chaperones involves a conserved interdomain linker. J. Biol. Chem. *281*, 38705–38711.

Weigelt, J. (1998). Single scan, sensitivity- and gradient-enhanced TROSY for multidimensional NMR experiments. J. Am. Chem. Soc. *120*, 10778–10779.

Wilbanks, S.M., Chen, L., Tsuruta, H., Hodgson, K.O., and McKay, D.B. (1995). Solution small-angle X-ray scattering study of the molecular chaperone Hsc70 and its subfragments. Biochemistry *34*, 12095–12106.

Zhu, X.T., Zhao, X., Burkholder, W.F., Gragerov, A., Ogata, C.M., Gottesman, M.E., and Hendrickson, W.A. (1996). Structural analysis of substrate binding by the molecular chaperone DnaK. Science *272*, 1606–1614.

Zhuravleva, A., and Gierasch, L.M. (2011). Allosteric signal transmission in the nucleotide-binding domain of 70-kDa heat shock protein (Hsp70) molecular chaperones. Proc. Natl. Acad. Sci. USA *108*, 6987–6992.

Note Added in Proof

While this article was in press, the X-ray crystal structure of DnaK in the ATP-bound state was reported by Kityk and coworkers. Their structure reveals that the NBD, β-SBD, and α-helical lid are arranged very similarly to the structure of Sse1 (Liu and Hendrickson, 2007) and are fully consistent with the results we report here for ATP-bound DnaK in solution, based on NMR analysis and soft mutations. Moreover, the conclusion reached by Kityk et al. using fluorescence methods that docking of the β-SBD and α-helical lid to the NBD is a sequential process and is consistent with our analysis of thermodynamic competition among interfaces formed by the NBD, β-SBD, and α-helical lid interdomain interactions. Kityk, R., Kopp, J., Sinning, I., and Mayer, M.P. (2012). Structure and dynamics of the ATP-bound open conformation of Hsp70 chaperones. Mol. Cell. Published online November 1, 2012. http://dx.doi.org/10.1016/j.molcel.2012.09.023.